Reptation with Configuration-Dependent Constraint Release in the Dynamics of Flexible Polymers

Hiroshi Watanabe[†] and Matthew Tirrell*

Department of Chemical Engineering and Materials Science, University of Minnesota, Minneapolis, Minnesota 55455. *Received April 22, 1988; Revised Manuscript Received August 8, 1988*

ABSTRACT: The effect of simultaneous reptation and tube deformation on the dynamic properties of polymers has been examined. We propose the configuration-dependent constraint release (CDCR) mechanism. The decay of the memory of the tube orientation is assumed to be governed by Rouse dynamics, and therefore the rate of tube deformation, or constraint release in our model, varies along the contour of the tube. This is in contrast with the type of model originally proposed by Graessley, where constraint release occurs uniformly along the chain contour. We reformulate Graessley's model in our terminology in order to make comparisons with our CDCR model. We examine two categories of situations. One is binary blends of polymers, with the longer components too dilute to entangle among themselves, where the effects of constraint release can be arbitrarily exaggerated and separated from reptation. The second is monodisperse polymers. For the blends in a constraint release dominant regime, relaxation of orientation in a polymer after a constant step strain occurs much less uniformly along the chain in the CDCR model than in Graessley's model. This difference could be sought experimentally. Overall, for CDCR the effect of constraint release competing with reptation is smaller than in the Graessley model under equivalent circumstances. One manifestation of this is in the prediction of the zero shear rate viscosity variation with molecular weight. CDCR overpredicts the experimental viscosity but goes asymptotically to pure reptation at high molecular weight where Graessley's model underpredicts the viscosity and does not go to the pure reptation limit. The self-diffusion coefficient obtained from our model is the same as that of the Graessley model, while the end-to-end vector correlation function is quite different: Our model predicts that the combination of constraint release and reptation processes shifts the characteristic time but does not change the distribution of the relaxation modes of this function, while the Graessley model predicts the change of the mode distribution due to the combination of these processes. This gives another method for the experimental examination of these models.

Introduction

The entanglement effect is one of the central problems in polymer physics, and many molecular theories have been developed to explain the dynamic properties of flexible polymer systems.[1-3] Among those theories, the Doi–Edwards (DE) theory[3,4] based on the concept of reptation has been widely used to describe various kinds of dynamic properties such as viscoelasticity,[3,5-7] diffusion,[3,6,7] polymer healing due to interdiffusion,[8] dielectric relaxation,[9,10] and so on. However, for some properties, the DE theory, in its original form, does not give a satisfactory explanation of several observations. For example, the relaxation time, τ, of entangled monodisperse polymers with the molecular weight, M, is predicted to be proportional to M^3, while the experimentally observed relation[1,2] is $\tau \propto M^{3.3-3.8}$.

In the framework of the generalized tube model, these kinds of disagreements have been attributed to the upper-bound nature of the reptation mechanism:[6] For monodisperse systems of linear chains, reptation is expected to be the only possible mechanism for infinitely long chains, since other competing mechanisms have much longer characteristic times and/or much smaller intensities. However, for dynamic properties of polymer chains having *finite* length, those competing mechanisms such as contour-length fluctuation (or path breathing)[6,11] and constraint release (or tube renewal)[6,12,13] would also contribute significantly. In particular, the importance of the constraint release mechanism appears to be well established experimentally for binary blends composed of monodisperse polymers having *widely* separated molecular weights.[14-25] In such *extreme* cases, the constraint release process is dominant, i.e., much faster than reptation. However, in general, for entangled polymers of moderate molecular weight, we should consider the contribution from both of these processes.

[†]Permanent address: Department of Macromolecular Science, Faculty of Science, Osaka University, Toyonaka, Osaka 560, Japan.

The effect of the combination of constraint release and reptation on dynamic properties such as relaxation modulus $G(t)$, was examined by Graessley,[6] who assumed those processes to be acting *independently* and hence $G(t)$ to be expressed as a simple product of reptation and constraint release terms. Thus, $G(t)$ was calculated without going through a detailed analysis of the orientation function, $S(n, t)$, which gives the orientation of the nth segment of the chain as a function of time during a relaxation process and can be related directly to the stress tensor as discussed by Pearson.[2]

The thrust of this paper is to propose an alternative model to Graessley's by which constraint release may compete with reptation. Instead of assuming that they are independent processes, *in the sense that the relaxation function can be expressed simply as the product of reptation and constraint release terms*, we go back and analyze the problem at the level of the orientation function. We assume that reptation and constraint release occur in parallel in the time-evolution equation for $S(n, t)$. Using the Rouse dynamics for the tube deformation, we have attempted to estimate the effect of the combination of constraint release and reptation mechanisms on $G(t)$ and some other dynamic properties. (Thus, in a sense, we are following through on the path *originally* conceived by Graessley,[6] who outlined the full problem on constraint release and then suggested the independent relaxation model.) In this paper, we present the results and compare the features of our model with those of the other models,[6,12] and also compare those models with experimental data. (Although contour length fluctuation is another important mechanism competing with reptation, especially for monodisperse systems, for simplicity, we do not incorporate its effect in our present model.)

Linear Viscoelasticity

In this section, we first describe the difference in the features of Graessley's model and our model and then compare the prediction of the models with experiments.

0024-9297/89/2222-0927$01.50/0

Theory. General Expression. We suppose that a *small* shear strain, γ, is imposed (in the x direction) at time $t = 0$ on a primitive chain[4] composed of N segments (with size a and segmental friction coefficient ζ_0) trapped in a tube. Let $\mathbf{r}(n, t)$ be the position of the nth segment at time t. Using the orientation function[4] defined by

$$S(n, t) = \langle u_x(n, t)u_y(n, t)\rangle/a^2 \tag{1}$$

with $u_\alpha(n, t)$ being the α ($=x, y$) component of the tangent vector $\partial\mathbf{r}(n, t)/\partial n$ at the nth segment and $\langle \dots \rangle$ representing the average over the ensemble of the primitive chains, we can describe the anisotropy of the conformation of primitive chains (hereafter simply designated as chain). Assuming a uniform deformation profile at $t = 0$ throughout the chain contour, we have, as the initial condition for S,

$$S(n,0) = S_0 = \begin{cases} 4\gamma/15 & \text{(2a)} \\ \gamma/3 & \text{(2b)} \end{cases}$$

Equation 2a is the initial condition for $\gamma \ll 1$ derived from Doi–Edwards theory,[3] in which the origin of time ($t = 0$) for the slow relaxation process (reptation) is chosen so that other fast relaxation processes have finished at $t = 0$. On the other hand, eq 2b is the initial condition obtained for an affine deformation[1] at $t = 0$. Though we use eq 2a in the following, the results obtained in this section, except for the reduced compliance cited in Table II, remain the same with the second initial condition eq 2b.

Using $S(n, t)$, we can write the relaxation (shear) modulus, $G(t)$, as

$$G(t) = G_0\mu(t) \tag{3}$$

where

$$\mu(t) = (1/NS_0)\int_0^N \mathrm{d}n\, S(n, t) \tag{4}$$

with G_0 and $\mu(t)$ being the plateau modulus and reduced relaxation modulus, respectively. All linear viscoelastic quantities of our interest can be evaluated from $G(t)$. Now we consider the time evolution of $S(n, t)$ due to constraint release and reptation taking place simultaneously. We begin by recasting the Graessley model in terms of the orientation function, $S(n, t)$, in a form that is *not* the one developed by Graessley, but is the one that we believe is fundamentally identical with his original presentation.[6]

Extended Graessley Model. If we assume **(assumption 1)** the rate constant for the constraint release to be the same throughout the chain contour, i.e., independent of the configuration of the tube, we reach the time-evolution equation

$$\partial S(n, t)/\partial t = D_c\, \partial^2 S(n, t)/\partial n^2 + k_{cr}(t)S(n, t) \tag{5}$$

Here, the first term represents the contribution of reptation, and D_c is given by $kT/a^2N\zeta_0$, with kT being the thermal energy and ζ_0 the segmental friction coefficient. The expression for the constraint release contribution (second term) is similar to that for a chemical reaction (with the rate constant $k_{cr}(t)$).

We may assume the tube to behave as a (hypothetical) Rouse chain composed of N tube segments with the friction coefficient ζ_t.[6,12] If we further assume **(assumption 2)** the rate constant, $k_{cr}(t)$, to be given by that for a *pure* constraint release process, we obtain

$$k_{cr}(t) = [\mathrm{d}\mu_{cr}(t)/\mathrm{d}t]/\mu_{cr}(t) \tag{6}$$

with

$$\mu_{cr}(t) = (1/N)[\sum_{q=1}^{N} \exp(-2D_t\lambda_q{}^2 t)] \tag{7}$$

and

$$\lambda_q = q\pi/N \qquad D_t = 3kT/a^2\zeta_t \tag{8}$$

(Note that our expressions for D_c and D_t differ from the normally used expression by a factor of $1/a^2$, since our equation is based on the segmental number n, not on the curvilinear distance along the chain contour.) Then, with the boundary condition[4]

$$S(n, t) = 0 \quad \text{at} \quad n = 0, N \qquad \text{(random orientation at chain ends)} \tag{9}$$

and the initial condition eq 2a, eq 5 gives

$$\begin{aligned} S(n, t) &= S_0\mu_{cr}(t)\tilde{S}_{rep}(n, t) \\ &= S_0\mu_{cr}(t)[\sum_{p=\text{odd}} (4/p\pi) \sin \lambda_p n \exp(-D_c\lambda_p{}^2 t)] \end{aligned} \tag{10}$$

with $\tilde{S}_{rep}(n, t)$ being the normalized orientation function for pure reptation, and

$$\mu(t) = \mu_{cr}(t)\mu_{rep}(t) \tag{11}$$

with

$$\mu_{rep}(t) = \sum_{p=\text{odd}} (8/p^2\pi^2) \exp(-D_c\lambda_p{}^2 t) \tag{12}$$

The reduced relaxation modulus, $\mu(t)$, obtained (eq 11) is identical with that proposed by Graessley,[6] who *assumed* the reptation and constraint release processes to be acting *independently*.

Based on the independence assumption mentioned above, Graessley proposed μ for the combined reptation plus constraint release process to be given by the product $\mu_{rep}\mu_{cr}$, because μ_{rep} and μ_{cr} can be interpreted as the probabilities that some initial tube segment has survived *on average* (taken throughout the chain contour) at time t for *pure* reptation and constraint release processes, respectively. For this argument to have a sound base, the same idea should be applied also to the reduced orientation function $S(n, t)/S_0$, since the physical meaning of this function is the probability that the initial tube *at the nth segment* has survived at time t. Namely, according to the Graessley assumption, $S(n, t)/S_0$ for the combined process should be given by the product of two $S(n, t)/S_0$ functions obtained for pure reptation and constraint release processes, respectively. We can easily see that the solution of eq 5 satisfies this requirement. (The two $S(n, t)/S_0$ functions for the two pure processes are obtained by putting either $D_c = 0$ or $k_{cr} = 0$ in eq 5.)

It is not certain that Graessley's assumption is equivalent to assumptions 1 and 2, since he derived eq 11 without using $S(n, t)$, as mentioned above. However, since $\mu(t)$ calculated from eq 5 agrees with his $\mu(t)$, and since eq 5 also leads to the solution which satisfies the requirement that $S(n, t)$ can be factored into reptation and constraint release functions, we may *assume* eq 5 to be the time-evolution equation for $S(n, t)$ of his model. Klein's model[12] for the constraint release plus reptation process also falls into this category. Hereafter, for simplicity, we designate this class of models based on assumptions 1 and 2 as the extended Graessley model and do not distinguish between the original and extended models unless necessary.

Assumptions 1 and 2 are certainly open for discussion. If the tube behaves strictly as a Rouse chain, the effective rate constant, k_{cr}, for the constraint release should depend on the configuration of the tube. In other words, that rate constant should be dependent on n. Thus, we propose an alternative set of assumptions (instead of 1 and 2) and reexamine the time evolution of $S(n, t)$.

Configuration-Dependent Constraint Release plus Reptation. Figure 1 shows schematically our molecular

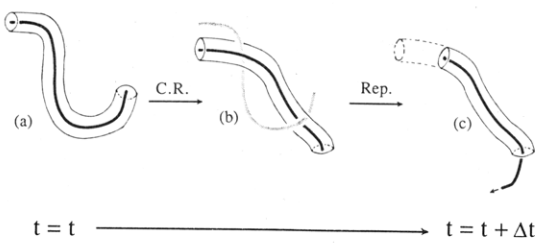

Figure 1. Schematic diagram representing the combined constraint release plus reptation process. During the short period of time Δt, the tube is allowed to deform first (from a to b), and then the chain (thick line) is allowed to reptate along this deformed tube (b to c).

picture. We again assume that the tube relaxes in a Rouse-like fashion,[6] and (**assumption 3**) during a short period of time, $t - (t + \Delta t)$, the relaxation takes place in two steps; i.e., the tube first deforms according to Rouse dynamics (from a to b in Figure 1) and then the chain (thick solid line in the tube) reptates along this deformed tube (from b to c in Figure 1). In this molecular picture, the rate constant of constraint release is dependent on the tube configuration. We designate this model as the CDCR (configuration-dependent constraint release) model.

The change of $S(n, t)$ during a short period of time, $t - (t + \Delta t)$, is obtained by the following procedure: First, the tube configuration at the end of the first step (constraint release; Figure 1b) is calculated from that at the beginning of the first step (Figure 1a). To do this, we can evaluate the amplitudes of the Rouse eigenfunctions contributing to $S(n, t)$ at time t and allow them to decay according to Rouse dynamics. Then, as the second step, the chain trapped in the deformed tube is allowed to reptate to obtain $S(n, t + \Delta t)$, the orientation function at $t + \Delta t$ for our model.

We see clearly in Figure 1 that the chain configuration at the beginning of the second step (reptation) is affected by the first one. Namely, in distinction to the Graessley model, the change of S during the period t to $t + \Delta t$ in our model cannot be represented by the product of the terms for pure constraint release and reptation processes, both of which are obtained from the same configuration at time t.

To obtain an analytic expression for the time-evolution equation, we further assume (**assumption 4**) that $S(n, t)$ is *approximated* during the first (constraint release) step by a linear combination of *diagonal* parts of the Rouse eigenfunctions $f_{qq}^{R} = \sin^2 \lambda_q n$ satisfying the boundary condition eq 9. In general, off-diagonal Rouse eigenfunctions $f_{pq}^{R} = \sin \lambda_p n \sin \lambda_q n$ $(q \neq p)$ could contribute to $S(n, t)$. As shown in Appendix A, the effect of the constraint release in such cases seems to be larger than that described by the present model (eq 19) with the diagonal dominance approximation. Thus, the relaxation time and the relaxation mode distribution obtained below, respectively, give the upper and lower bound for general cases.

With the diagonal dominance approximation (assumption 4), we may write

$$S(n, t) = \sum_{q=1}^{N} A_{qq}^{R}(t) f_{qq}^{R}(n) \tag{13}$$

Using the orthogonality relation for the diagonal eigenfunctions,

$$\int_0^N dn\, f_{pp}^{R}(n) f_{qq}^{R}(n) - (1/N)\left\{\int_0^N dn\, f_{pp}^{R}(n)\right\}\left\{\int_0^N dn\, f_{qq}^{R}(n)\right\} = (N/8)\delta_{pq}$$

with δ_{pq} being the Kronecker's delta, we obtain the amplitude, A_{qq}^{R}, of the eigenfunction, f_{qq}^{R}, as

$$A_{qq}^{R} = (8/N)\left[\int_0^N dn\, S(n, t) f_{qq}^{R}(n) - (1/N)\left\{\int_0^N dn\, S(n, t)\right\}\left\{\int_0^N dn\, f_{qq}^{R}(n)\right\}\right] = (-4/N)\int_0^N dn\, S(n, t) \cos 2\lambda_q n \tag{14}$$

(For off-diagonal eigenfunctions, this sort of orthogonality relation cannot be found; thus, our use of the diagonal dominance approximation was necessitated.)

As described above, this amplitude should decay, due to tube deformation during a period of time Δt, by a factor of $\exp(-2D_t\lambda_q^2\Delta t)$, i.e.,

$$A_{qq}^{R}(t+\Delta t) = \exp(-2D_t\lambda_q^2\Delta t) A_{qq}^{R}(t) \tag{15}$$

and we have, after constraint release (Figure 1b),

$$S_{\text{tube}} = \sum_{q=1}^{N} \exp(-2D_t\lambda_q^2\Delta t) A_{qq}^{R}(t) \sin^2 \lambda_q n \tag{16}$$

The reptation eigenfunction, $f_p^{\text{rep}} = \sin \lambda_p n$ (for the boundary condition eq 9), contributing to S_{tube} has the amplitude

$$A_p^{\text{rep}} = (2/N)\int_0^N dn\, S_{\text{tube}} \sin \lambda_p n \tag{17}$$

which should decay by a factor of $\exp(-D_c\lambda_p^2\Delta t)$ during Δt due to successive reptation (from b to c in Figure 1). Thus, we obtain, after Taylor expansion with respect to Δt and integration by parts,

$$\begin{aligned} S(n, t+\Delta t) &= \sum_p A_p^{\text{rep}} \exp(-D_c\lambda_p^2\Delta t) \sin \lambda_p n = \\ &S(n, t) + D_c\Delta t(2/N)\sum_p \lambda_p^2 \sin \lambda_p n\left[\int_0^N dn' \sin \lambda_p n' \times \left\{(4/N)\sum_{q=1}^{N} \sin^2 \lambda_q n' \int_0^N dn''\, S(n'', t) \cos 2\lambda_q n''\right\}\right] + \\ &D_t\Delta t(2/N)\sum_p \sin \lambda_p n\left[\int_0^N dn' \sin \lambda_p n' \left\{(4/N) \times \sum_{q=1}^{N} 2\lambda_q^2 \sin^2 \lambda_q n' \int_0^N dn''\, S(n'', t) \cos 2\lambda_q n''\right\}\right] + \\ &O(\Delta t^2) = S(n, t) + \\ &\Delta t\left[(D_c + (1/2)D_t)\, \partial^2 S(n, t)/\partial n^2 + D_t\{\partial S(n', t)/\partial n'|_{n'=N} - \partial S(n', t)/\partial n'|_{n'=0}\} - D_t\int_0^N dn'\, (1/N) \times \sum_{q=1}^{N} \cos 2\lambda_q n'\, \partial^2 S(n', t)/\partial n'^2\right] + O(\Delta t^2) \end{aligned} \tag{18}$$

and, at the limit $\Delta t \to 0$, we reach the time-evolution equation[26]

$$\begin{aligned} (1/D)\, \partial S(n, t)/\partial t &= [1 - (w/2)]\, \partial^2 S(n, t)/\partial n^2 + \\ &w\left[(1/2)\, \partial^2 S(n, t)/\partial n^2 - \int_0^N dn'\, Q(n')\, \partial^2 S(n', t)/\partial n'^2 - \partial S(n', t)/\partial n'|_{n'=0} + \partial S(n', t)/\partial n'|_{n'=N}\right] \end{aligned} \tag{19}$$

with

$$D = D_c + (1/2)D_t \qquad w = 2D_t/(2D_c + D_t)$$
$$Q(n) = (1/N)\sum_{q=1}^{N} \cos 2\lambda_q n \tag{20}$$

Note that the same time-evolution equation is obtained even if we assume that reptation takes place first and then

constraint release follows (cf., assumption 3).

Equation 19 indicates that the decay rate, $\partial S/\partial t$, is the sum of the contribution from reptation and constraint release, both of which are tube configuration dependent in our model. Note that the expression for the constraint release contribution (second term) is that for a diffusion process, differing from that in the extended Graessley model, eq 5.

The solution of eq 19 for $N \gg 1$ under the initial and boundary conditions given by eq 2a and 9 can be found by the eigenfunction expansion method. As shown in Appendix B, we obtain

$$S(n, t) = S_0 \sum_{p=1}^{N} B_p\{\cos [\theta_p(2n - N)/N] - \cos \theta_p\} \exp[-D(2\theta_p/N)2^t] \quad (21)$$

with

$$B_p = -Bw(2N + 1) \cos \theta_p/[w(2N + 1) + (2 - w) \cos^2 \theta_p] \qquad p = 1, 2, ..., N \quad (21')$$

$$B = [[w(2N + 1) + (2 - w)] \times \sum_{k=1}^{N} \{\cos^2 \theta_k/[w(2N + 1) + (2 - w) \cos^2 \theta_k]\}]^{-1} \quad (21'')$$

and

$$\tan \theta_p = [(w - 2)/w]\theta_p/(2N + 1) = -(2D_c/D_t)\theta_p/(2N + 1) \qquad p = 1, 2, ..., N \quad (22)$$

One interesting feature of eq 21 is as follows: From the eigenvalue equation, eq 22, we see θ_p approaches $(p - 1/2)\pi$, and hence, the eigenfunction, $B_p\{\cos [\theta_p(2n - N)/N] - \cos \theta_p\}$, approaches $[4/(2p - 1)\pi] \sin [(2p - 1)\pi n/N]$, the reptation limit, with increasing p. Namely, the effect of constraint release described by our model is less prominent for higher order normal modes, i.e., for shorter times.

From eq 21, the reduced relaxation modulus is calculated as

$$\mu(t) = \sum_{p=1}^{N} B'_p \exp[-D(2\theta_p/N)^2 t] \quad (23)$$

with

$$B'_p = -[1 + (2 - w)/w(2N + 1)]B_p \cos \theta_p \quad (23')$$

We may characterize $G(t) = G_0\mu(t)$ by the longest relaxation time

$$\tau_1 = (N/2\theta_1)^2/[D_c + (1/2)D_t] \quad (24)$$

the zero-shear viscosity

$$\eta = \int_0^\infty dt\, G(t) = (N^2G_0/4D) \sum_{p=1}^{N} B'_p/\theta_p^2 \quad (25a)$$

and the recoverable compliance

$$J_e = \int_0^\infty dt\, tG(t)/\left[\int_0^\infty dt\, G(t)\right]^2 = (1/G_0)[\sum_{p=1}^{N} B'_p/\theta_p^4]/[\sum_{p=1}^{N} B'_p/\theta_p^2]^2 \quad (25b)$$

The product J_eG_0 gives a measure for the polydispersity of the relaxation mode distribution.

Using the reptation time, $\tau_{rep} = (N/\pi)^2/D_c$, and constraint release (tube renewal) time, $\tau_{tube} = (N/\pi)^2/2D_t$, eq 24 can be rewritten as

$$\tau_1 = (\pi/2\theta_1)^2/[\tau_{rep}^{-1} + (1/4)\tau_{tube}^{-1}] \quad (24')$$

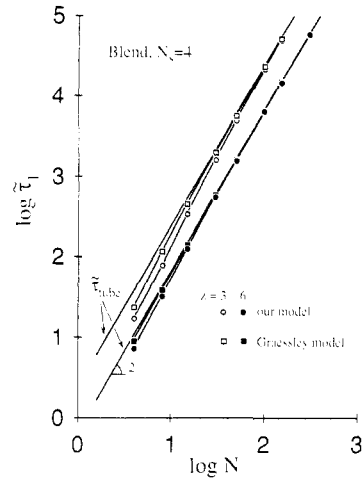

Figure 2. N dependence of the relaxation time of the N-mer (dilute component) in blends with short N_s-mers. The circles indicate the results of our model and squares those of the Graessley model. The parameters used are $N_s = 4$, $z = 3$ and 6. (z is a parameter in Graessley's model, giving the number of local jump sites for a chain segment.)

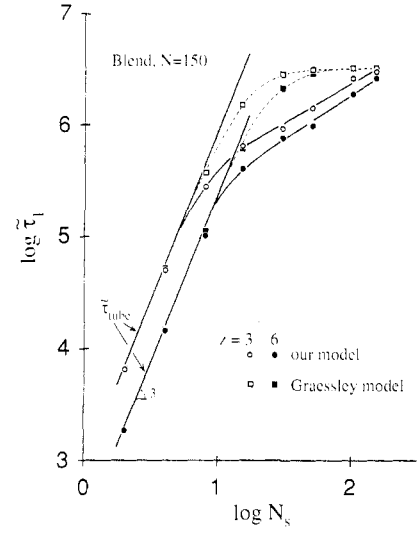

Figure 3. N_s dependence of the relaxation time of the N-mer (dilute component) in the blends. The circles indicate the results of our model and squares those of the Graessley model. The parameters used are $N = 150$, $z = 3$ and 6.

At the asymptotic limits $D_t \to 0$ and $D_c \to 0$, θ_1 approaches $\pi/2$ and π (cf., eq 22), and hence, τ_1 approaches τ_{rep} and τ_{tube}, respectively. $S(n, t)$ (eq 21) also recovers the aymptotic forms in those limits, as shown in Appendix B.

Comparison of CDCR Model and Extended Graessley Model. To estimate the relative magnitudes of D_t and D_c, we assume that the tube confining the chain (N-mer) is composed of N_s-mers. Namely, we consider a very *dilute* N-mer component in N_s-mers. Furthermore, in order to make direct contact with Graessley's model, the motion (local jump) of tube sugments is assumed to be due to reptation (or diffusion) of N_s-mers. Specifically, assuming Graessley's local jump model,[6] we have

$$\zeta_t = 12\Lambda(z)\zeta_0 N_s^3/\pi^2 \qquad D_t = \pi^2 N D_c/[4\Lambda(z)N_s^3] \quad (26)$$

where $\Lambda(z) = (\pi^2/12)^z/z$ is a constant determined by the number z of the local jump gates per one tube segment. In the following, we compare the features of our CDCR model with those of the Graessley model, using identical values of the Graessley parameters shown in eq 26.

Dilute Blends with $N > N_s$. Figures 2 and 3 compare the relaxation time (in the form of reduced time, $\tilde{\tau}_1 =$

Table I
θ_p/π (p = 1-3) Obtained for the CDCR Model for N-mer in Dilute Blends[a]

p	N_S = 2	N_S = 4	N_S = 8	N_S = 15	N_S = 30	N_S = 50	N_S = 100
				N = 150, z = 3			
1	0.999 97	0.999 79	0.998 30	0.988 89	0.919 15	0.752 56	0.554 36
2	1.999 95	1.999 57	1.996 60	1.977 81	1.846 95	1.638 97	1.519 99
3	2.999 92	2.999 36	2.994 90	2.966 78	2.787 69	2.591 35	2.512 11
				N = 150, z = 6			
1	0.999 99	0.999 94	0.999 53	0.996 88	0.975 64	0.899 35	0.654 03
2	1.999 99	1.999 88	1.999 05	1.993 77	1.951 56	1.814 30	1.568 67
3	2.999 98	2.999 82	2.998 58	2.990 65	2.928 02	2.749 94	2.542 77

[a] Determined by eq 22.

$\pi^2 kT\tau_1/a^2\zeta_0$) of the N-mer in the blend predicted by our model (eq 24 and 24') and the Graessley model (cf., eq 10)[27]

$$\tau_1 = 1/[\tau_{rep}^{-1} + \tau_{tube}^{-1}] \quad \text{(Graessley model)} \quad (27)$$

The Graessley parameters used are z = 3 (Λ = 0.185) and z = 6 (Λ = 0.0516). For convenience, some of the low-order eigenvalues of our model are given in Table I.

In Figure 2, we see that τ_1 for both our model (circles) and the Graessley model (squares) is close to τ_{tube} ($\propto N^2$) for $N \gg N_s$ (N_s = 4 in Figure 2). The asymptotic constraint release dominant region (where $\tau_1 \propto N^2$) is reached more easily for larger z (filled symbols). As N approaches N_s, τ_1 deviates downward from τ_{tube} and its N dependence becomes stronger, due to the reptation contribution. The difference between the two models is not particularly evident in this figure. (Note that, for actual polymer systems, τ_1 finally approaches the intrinsic Rouse relaxation time ($\propto \zeta_0 N^2 N_s^0$). Thus, the asymptotic N dependence of τ_1 for very small N is again given by N^2.)

In Figure 3, we again see that τ_1 predicted by the two models agrees with τ_{tube} ($\propto N_s^3$) for $N \gg N_s$, i.e., $D_t \gg D_c$. However, as N_s approaches N (=150 in this Figure), τ_1 of our model deviates downward from τ_{tube} much earlier than τ_1 of the Graessley model. This deviation is observed at smaller N_s for smaller z (unfilled symbols). Thus, for the longest relaxation time of the N-mer in the blend, the effect of reptation competing with constraint release is larger in our model.[28] We also note that τ_1 for the Graessley model for this large N (=150) is independent of N_s in a fairly wide range of N_s, while our model predicts τ_1 to be increasing with N_s even for N_s close to N.

As seen in eq 25b, the recoverable compliance, J_e, is sensitive to the relaxation mode distribution, and it is informative to examine its behavior in relation to τ_1. Table II summarizes the reduced compliance of the N-mer in the blend

$$J_e^R = (cRT/M)J_e \quad (28)$$

predicted by the two models. Here, c is the mass of the N-mer (with the molecular weight M) in unit volume, and we used the Doi-Edwards relation $G_0 = 4cRT/5M_e = (M/M_e)(4cRT/5M) = N(4cRT/5M)$ to calculate J_e^R from J_e.

As shown in Table II, both models give J_e^R ($\simeq$0.5) being independent of N_s for $N \gg N_s$.[29] Namely, the relaxation mode distribution is universal and independent of N_s in that extreme region where J_e^R is constant. On the other hand, J_e^R decreases as N_s approaches N, implying the change in the relaxation mode distribution. This decrease in J_e^R is observed at smaller N_s in our model than in the Graessley model, corresponding to the deviation of τ_1 from τ_{tube} shown in Figure 3.[30]

The essential difference between our CDCR model and the extended Graessley model is much more clearly observed for the orientation function $S(n, t)$ (eq 10 and 21).

Table II
Reduced Compliance, J_e^R, of N-mer in Dilute Blends[a]

N_s	this work	Graessley model
	z = 6	
2	0.504	0.505
4	0.504	0.505
8	0.496	0.501
15	0.336	0.471
30	0.072	0.296
50	0.024	0.153
100	0.012	0.058
	z = 3	
2	0.504	0.505
4	0.502	0.504
8	0.426	0.489
15	0.139	0.383
30	0.028	0.172
50	0.014	0.084
100	0.010	0.033

[a] The parameters used are N = 150; the Doi-Edwards relation $G_0 = 4cRT/5M_e$ was used to calculate J_e^R.

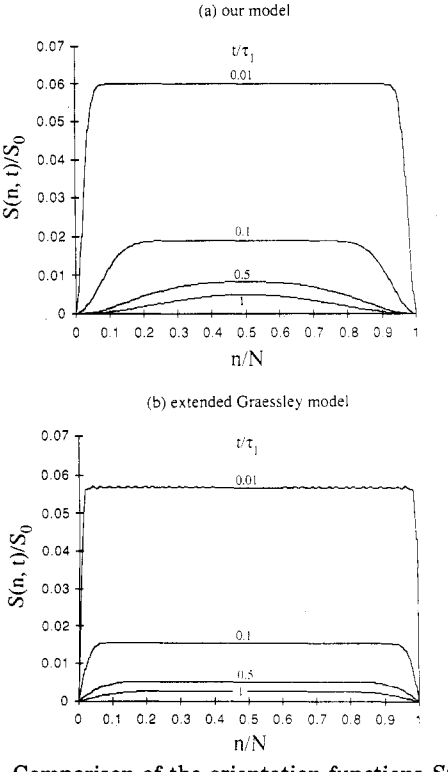

Figure 4. Comparison of the orientation functions $S(n, t)$ for the N-mer (dilute component) in the blend predicted by (a) our model (eq 21) and (b) the extended Graessley model (eq 10). The parameters used are N = 150, N_s = 8, and z = 6.

Figure 4 compares the orientation distributions along the chain predicted by the two models at various fractions of the longest relaxation time: t/τ_1 = 0.01, 0.1, 0.5, and 1. The parameters used are N = 150, N_s = 8, and z = 6. As

Table III
θ_p/π (p = 1–3) Obtained for the CDCR Model for Monodisperse Systems[a]

p	N = 10	N = 20	N = 30	N = 50	N = 80	N = 150
			z = 3			
1	0.683 57	0.608 97	0.577 52	0.549 18	0.531 78	0.517 41
2	1.586 95	1.544 44	1.529 77	1.517 92	1.511 21	1.505 99
3	2.554 85	2.527 27	2.518 12	2.510 84	2.506 76	2.503 60
			z = 6			
1	0.845 19	0.755 41	0.701 87	0.642 44	0.598 61	0.557 42
2	1.736 82	1.641 44	1.599 39	1.562 04	1.539 42	1.521 24
3	2.671 64	2.593 18	2.563 27	2.538 48	2.524 12	2.512 80

[a] Determined by eq 22.

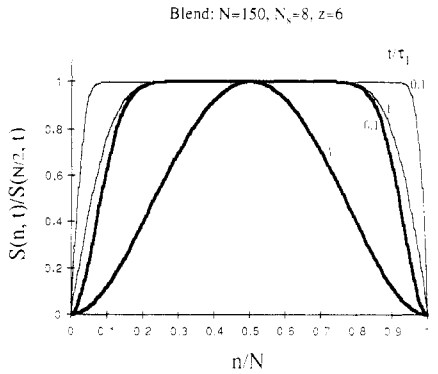

Figure 5. Comparison of the reduced orientation function $S(n, t)/S(N/2, t)$ for the N-mer in the blend predicted by our model (thick lines) and the extended Graessley model (thin lines). The parameters used are the same as in Figure 4.

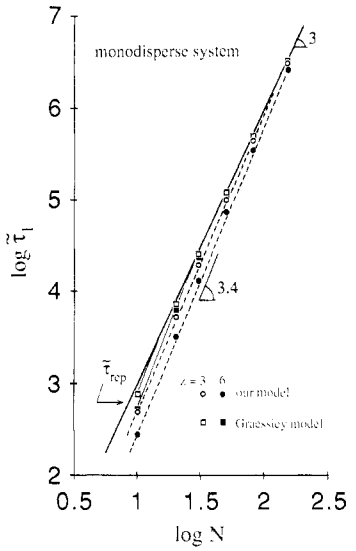

Figure 6. N dependence of the relaxation time for monodisperse systems. The circles indicate the results of our model and squares those of the Graessley model. The parameters used are z = 3 and 6.

can be seen from Figure 3 and Table II, for those parameters, the calculated results are well in the universal (constraint release-dominant) region where J_e is independent of N_s and τ_1 is very close to τ_{tube} ($\propto N_s^3$).

In Figure 4, for both models, we first note that the decay of the orientation (decrease in S) takes place rapidly (i.e., even at $t = \tau_1/100$) not only at the chain ends but also at the middle part of the chain contour, in contrast to the behavior of S for the pure reptation mechanism. However, we also note that the $S(n, t)$ profile is flatter, i.e., the strain is distributed throughout the chain contour more uniformly in the extended Graessley model than in our model.

This feature is more closely observed in Figure 5, where we compare the profiles $S(n, t)/S(N/2, t)$ reduced at the center of the chain. In the asymptotic limit ($N \gg N_s$), we see that the $S(n, t)$ profile of the extended Graessley model is completely flat in the entire range of time, because $\tilde{S}_{rep}(n, t)$ in eq 10 is unity for $0 < n < N$ even at $t \geq \tau_1$. On the other hand, in that limit, our model predicts $S(n, t)$ to become proportional to $\sin^2(\pi n/N)$, the first-order Rouse eigenfunction, at long times.

This suggests some means to distinguish the two models experimentally by optical methods, such as birefringence during stress relaxation. Using block copolymer molecules (N-mers) having various compositions and architectures (i.e., diblock or triblock) and being uniformly dissolved in a high excess of constituent homopolymers (N_s-mers), one could observe the orientation of the middle (or end) part of the dilute block copolymer chains by the birefringence method.

For blends composed of matrix N_s-mers and dilute N-mers with the volume fractions φ_S and φ_L ($\ll\varphi_S$), respectively, and a plasticizer with the volume fraction $1 - \varphi_p$ (φ_p ($\varphi_p = \varphi_S + \varphi_L$), $= \varphi_S + \varphi_L$), both the CDCR model and the Graessley model lead to a blending law for the reduced relaxation modulus

$$\mu_B(t) = [\varphi_S\mu_{S,B}(t) + \varphi_L\mu_{L,B}(t)]/\varphi_p \quad (\text{for } \varphi_L \ll \varphi_S) \quad (29)$$

where $\mu_{S,B}$ and $\mu_{L,B}$ are the reduced relaxation moduli of N_s- and N-mers *in the blend*, respectively (note that $\varphi_S\mu_{S,B}(t) + \varphi_L\mu_{L,B}(t) = \varphi_p$ at $t = 0$): For our model, $\mu_{L,B}$ is already given by eq 23. $\mu_{S,B}$ can be replaced by $\mu_{S,m}$ for the monodisperse N_s-mers (given by eq 23 with $N = N_s$), because the behavior of N_s-mers in the blends with $\varphi_L \ll \varphi_S$ should be very close to that in the monodisperse system. Similarly, $\mu_{L,B}$ and $\mu_{S,B}$ for the Graessley model are given by eq 11.

We should emphasize that eq 29 is the blending law for dilute blends in which N-mer is entangled only with N_s-mers. Recently, Rubinstein et al.[31] proposed a blending law for general cases in whith N-mers themselves are also entangled with one another. Although they did not use the time-evolution equation of $S(n, t)$ in their theory, their blending law might be derived from the molecular picture of uniform constraint release (for S) as we showed earlier for the extended Graessley model. Thus, we expect that our CDCR model extended to general cases would give a blending law considerably different from their result.

In thinking about generalizations of our model, we note that the entanglements between N-mers themselves have lifetimes longer than those of entanglements between N- and N_s-mers. One possible way to incorporate this feature in our model is to use modified Rouse dynamics[1] (for which the friction coefficient, ζ_t, is not the same for all segments) for the tube deformation. We shall consider this extension in future work.

Monodisperse Systems. Figure 6 compares the reduced relaxation time for monodisperse systems ($N = N_s$) predicted by the CDCR and Graessley models. The pa-

Table IV
Product J_eG_0 for Monodisperse Systems Predicted by Our CDCR Model and the Graessley Model

N	this work	Graessley model
	$z = 6$	
10	1.942	3.514
20	1.632	3.974
30	1.497	4.039
50	1.383	4.063
80	1.315	4.067
150	1.262	4.067
	$z = 3$	
10	1.408	2.431
20	1.314	2.468
30	1.278	2.468
50	1.247	2.464
80	1.230	2.461
150	1.216	2.459

rameters used are $z = 3$ ($\Lambda = 0.185$) and $z = 6$ ($\Lambda = 0.0516$). For convenience, some of the eigenvalues of our model are given in Table III.

As can be seen clearly from Figure 6, the relaxation time of our model is smaller than that of the Graessley model and approaches the reptation limit more slowly. If we attempt to *approximate* the N dependence of τ_1 in this figure by a power-law relation (broken lines in the figure), we obtain $\tau_1 \propto N^{3.2}$ for $z = 3$ and $\tau_1 \propto N^{3.4}$ for $z = 6$ in the region $10 < N < 100$. (The extra 0.2-th and 0.4-th powers mostly come from the change of θ_1 with N shown in Table III.) Thus, for the relaxation time of monodisperse systems, the effect of constraint release is *larger* in our model than in the Graessley model.

Table IV shows the product J_eG_0 for the two models. We note that this product is larger in the Graessley model, and prediction of our model is still smaller than the experimentally observed value[1,2] (=2–3) even for $z = 6$. Apart from this difference, the most important difference between the two models is the asymptotic value of J_eG_0 for $N \gg 1$. In our model, the dynamics of the chain becomes identical with reptation dynamics (i.e., the tube deformation becomes extremely slow) in that limit, and J_eG_0 approaches the reptation value (=6/5). On the other hand, in the Graessley model, J_eG_0 approaches a value larger than the reptation value, because the higher order terms in the constraint release contribution ($\exp(-2D_t\lambda_q^2 t)$ in eq 7 with $q \sim N$) have characteristic times with their orders of magnitude comparable to τ_{rep}.

As we see later in Figure 12, a similar difference between the two models is found also for viscosity. Namely, in our model, the viscosity, η, of a monodisperse system slowly approaches the reptation limit. On the other hand, in Graessley's model, η rather rapidly approaches the asymptotic value which is proportional to N^3 but still smaller than the reptation limit.

The essential difference between the two models can be again observed for the orientation function $S(n, t)$. As can be seen from Figure 7, at early stages of stress relaxation ($t/\tau_1 = 0.01, 0.1$), the orientation (strain) is more concentrated at the middle part of the chain in the extended Graessley model, while the opposite is observed at late stages ($t = \tau_1$). As mentioned for blends, the two models could be distinguished experimentally by optical methods sensitive to orientation of different parts of a chain.

Comparison of Models and Experiments. Dilute Blends with $M > M_s$. In this section, we compare the empirical data for the polystyrene (PS) blends availabile in the literature[16,18] with the predictions of our CDCR model and the Graessley model. To do this, we need to evaluate the viscoelastic quantities (such as viscosity) of

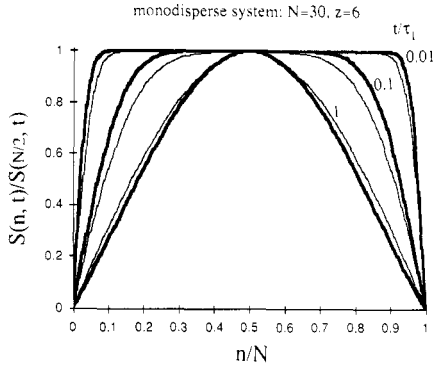

Figure 7. Comparison of the reduced orientation function $S(n, t)/S(N/2, t)$ predicted by our model (thick lines) and the extended Graessley model (thin lines) for the monodisperse system with $N = 30$. The parameter used is $z = 6$.

dilute and longer chains placed in the blend from the empirically determined quantities as follows.[15,16]

Evaluation of Experimental Quantities for the Longer Chain. Suppose a blend composed of shorter and longer chains (with the content φ_S and φ_L; $\varphi_S + \varphi_L = \varphi_p$) and plasticizer (or solvent, with the content $1 - \varphi_p$). For the *dilute* blend with $\varphi_S \gg \varphi_L$, irrespective of the molecular mechanism of relaxation, the behavior of the matrix (shorter) chains is identical with that in their monodisperse system, and the dynamics of the longer chain is independent of φ_L (e.g., relaxation time $\propto \varphi_L^0$ and relaxation intensity $\propto \varphi_L$). This enables us to evaluate the contribution of the longer chain to the complex modulus (at angular frequency ω) by

$$G^*_{L,B}(\omega) = G^*_B(\omega) - [\varphi_S G^*_{S,m}(\omega)/\varphi_p] \quad (30a)$$

and similarly, the contribution of the longer chain to the viscosity, elastic coefficient, and compliance by

$$\eta_{L,B} = \eta_B - [\varphi_S \eta_{S,m}/\varphi_p] \quad (30b)$$

$$A_{L,B} = A_B - [\varphi_S A_{S,m}/\varphi_p] \quad (30c)$$

$$J_{L,B} = A_{L,B}/(\eta_{L,B})^2 \quad (30d)$$

where the subscripts B and S,m represent the *empirically determined* quantities for the blend and (plasticized) monodisperse system of the shorter chain with the concentration φ_p.

It is clear that these expressions are essentially the same as those for dilute solutions. In fact, for dilute blends in which no entanglements between the longer chains exist, it has been experimentally observed[15,18] that

$$\eta_{L,B} \propto \varphi_L \qquad A_{L,B} \propto \varphi_L \qquad J_{L,B} \propto \varphi_L^{-1} \quad (30e)$$

In other words, whenever we observe φ_L dependence of $\eta_{L,B}$, $A_{L,B}$, and $J_{L,B}$ stronger than that described by eq 30e, this is a sign that the longer chains in the blend are entangled among themselves.[32]

Test of the Models. One of the most critical tests for our model and the Graessley model would be to compare the prediction of the models with data for storage moduli, $G'_{L,B}(\omega)$, of the long chain in the blend (eq 30a): $G'_{L,B}$ is very sensitive to the distribution of slow relaxation modes. That is, it is sensitive to the change of the contribution of constraint release to the relaxation process.

For both of the two models, we can write $G'_{L,B}(\omega)$ as

$$G'_{L,B}(\omega) = \omega \int_0^\infty dt \sin \omega t [G_0^\circ \varphi_L \mu_{L,B}(t)] \quad (31)$$

where $\mu_{L,B}(t)$ is given by eq 23 and 11 for our model and

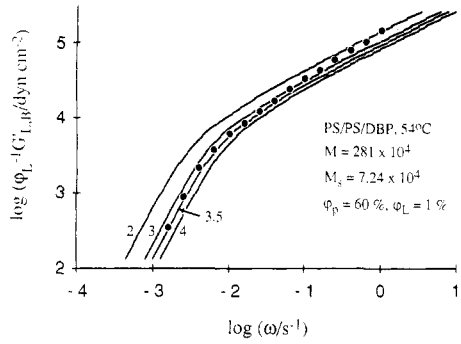

Figure 8. Comparison of $G'_{L,B}/\varphi_L$ curves (solid lines) predicted by our CDCR model with the data[16,18] (circles) for the longer chain ($M = 281 \times 10^4$, $\varphi_L = 1\%$) in the PS/PS/DBP blend with $M_s = 7.24 \times 10^4$ and $\varphi_p = 60\%$ at 54 °C. The numbers in the figure represent z values. For this system, the predicted curves are the same for our model and the Graessley model.

Graessley's model, respectively, and $G_0°$ is the plateau modulus reduced to $\varphi_p = 1$

$$G_0° = 4\rho RT/5M_e(\varphi_p) \qquad \text{(Doi–Edwards expression)} \tag{32}$$

Here, ρ and $M_e(\varphi_p)$ ($\propto \varphi_p^{-1}$ in concentrated systems) are the density and entanglement spacing of the blend, respectively, and we assumed $\rho\varphi_L$ to be equal to the mass of the long chain per unit volume.

To compare the empirical and theoretical $G'_{L,B}(\omega)$ in a quantitative fashion, we used the empirical data for the viscosity, $\eta(M_c)$, of the monodisperse system having the characteristic molecular weight, M_c ($= 3.2 \times 10^4/\varphi_p$ for PS), and plateau modulus, G_0. Using the Rouse relation, $\eta(M_c) = 5G_0a^2\zeta_0N_c/144kT$ with $N_c = M_c/M_e$, for the $\eta(M_c)$ and G_0 data, we evaluated the friction factor, $F_\zeta = a^2\zeta_0/kT = 144\eta(M_c)/5G_0N_c$, from which D_c was calculated as

$$D_c = 1/F_\zeta N \qquad N = M/M_e \tag{33}$$

Thus, the only free parameter remaining is the Graessley parameter, z.

To evaluate z for a series of blends with the same M, we chose the blend having the smallest M_s (which is *sufficiently* smaller than M but still larger than M_c) as a standard system, in which constraint release should become a dominant mechanism. For that system, we fit the empirical $G'_{L,B}(\omega)$ curve with the theoretical ones to determine the best z parameter.

As an example, Figure 8 shows this curve-fitting procedure for a reduced modulus, $G'_{L,B}(\omega)/\varphi_L$, of longer PS chains ($M = 281 \times 10^4$, $\varphi_L = 1\%$) in a blend containing 40% dibutyl phthalate (DBP) as a plasticizer (i.e., $\varphi_p = 60\%$). M_s for the matrix chain is 7.24×10^4. On the basis of the Doi–Edwards expression for the plateau modulus, we used $M_e = 1.44 \times 10^4/\varphi_p$ for the calculation of the theoretical curve. For the blend examined in this figure, $G'_{L,B}(\omega)$ was very close to $G'_B(\omega)$, because $G'_B(\omega)$ is insensitive to the fast relaxation of the matrix chains.

As can be seen from Figure 8, the theoretical curve predicted by our model with $z = 3.5$ fits the data (circles) well at low ω. (The curves predicted by our model and Graessley's model were indistinguishable for the z values examined here.) Thus, this parameter value, $z = 3.5$, was used also for the other blends with larger M_s in that series, as shown in Figure 9.

Figure 9 compares the experimental data (circles) for the PS/PS/DBP blends reported by Watanabe et al.[16,18] and the predictions of the models. The content, φ_L, of the longer chain ($M = 281 \times 10^4$) is 1% for all blends, and no

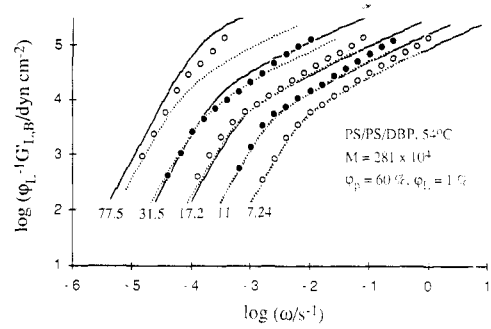

Figure 9. Comparison of the $G'_{L,B}/\varphi_L$ curves predicted by our CDCR model (solid lines) and the Graessley model (dotted lines) ($z = 3.5$) with the data (circles) for the longer chain[16,18] ($M = 281 \times 10^4$, $\varphi_L = 1\%$) in the PS/PS/DBP blends with $\varphi_p = 60\%$ at 54 °C. The numbers in the figure indicate $10^{-4}M_s$ for matrix PS.

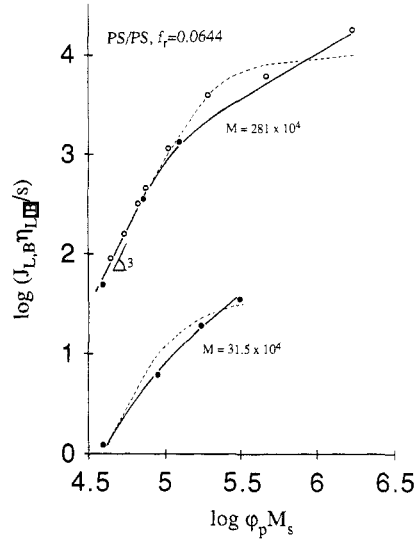

Figure 10. Comparison of the data[15,16,18] for the relaxation time of the dilute, longer chain in PS/PS/DBP blends with the prediction of our CDCR model (solid lines) and the Graessley model (dotted lines). The filled and unfilled circles are the data for blends with $\varphi_p = 100\%$ (melt) and 60%, respectively. All data were reduced at an iso-friction state ($f_r = 0.0644$) and plotted against the reduced molecular weight, φ_pM_s, of matrix PS.

entanglements between the longer chains exist. (The relation eq 30e was satisfied for $\varphi_L \leq 1\%$ and $M = 281 \times 10^4$.[15])

As can be seen from Figure 9, our CDCR model (solid lines) and Graessley's model (dotted lines) give undistinguishable curves which agree well with the data (circles) for the blends with $M \gg 17.2 \times 10^4 \geq M_s$, but the difference between the models becomes prominent for larger M_s. In particular, the shape of the two theoretical curves is entirely different for the blend having the highest M_s ($=77.5 \times 10^4$): Graessley's model still exhibits a Rouse wedgelike shoulder at $\log \omega > -4$, while our model does not; i.e., the change of the shape of the $G'_{L,B}(\omega)$ curve is less prominent for the Graessley model. From this viewpoint, our CDCR model appears to be in somewhat better (or at least equally good) agreement with the data shown here. Similar quality of agreement between the theoretical $G'_{L,B}(\omega)$ curves and data was found also for PS/PS *dilute* blends in the melt state.[15]

Here, we should again emphasize that both our model and Graessley's model are models only for dilute blends containing no entanglements between longer chains. In fact, we found that neither the Graessley model nor our model could give a good fit for $G'_{L,B}(\omega)$ of a series of PS/PS blends with $M = 270 \times 10^4$ and $\varphi_L = 2\%$ reported by Montfort et al.,[19] in which longer chains appear to be

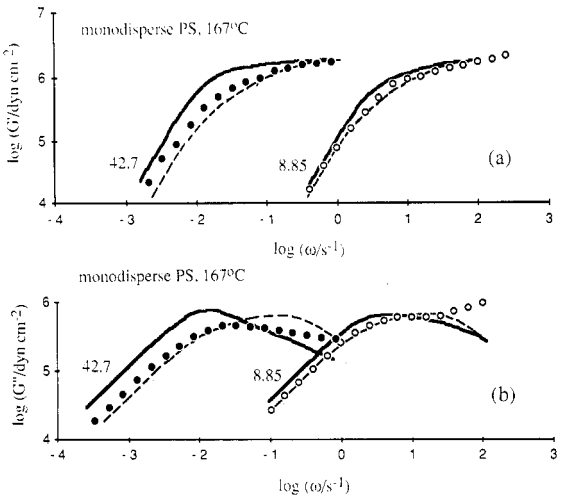

Figure 11. Comparison of (a) storage and (b) loss moduli of monodisperse melt PS at 167 °C[15] (circles) with the prediction of our CDCR model (solid lines) and the Graessley model (dotted lines). The Graessley parameter used was $z = 3.5$. The numbers in the figure indicate $10^{-4}M$ of PS.

entangled with themselves to some extent.[33]

Figure 10 compares the data[15,16,18] (circles) for the weight-average relaxation time, $J_{L,B}\eta_{L,B}$, of the longer chain in the blend with the predictions of our model (solid lines) and the Graessley model (dotted lines). All data are reduced at an iso-friction state with the free volume fraction $f_r = 0.0644$ and plotted against the reduced molecular weight, $\varphi_p M_s$ ($\propto M_s/M_e$), of the matrix chain. As in the case of τ_1 (see Figure 3), for small M_s, the weight-average relaxation time of the Graessley model is strongly dependent on M_s, while for large M_s, it is insensitive to M_s in a relatively wide range of M_s. On the other hand, the relaxation time of our model is still increasing gradually with M_s even at the vicinity of M. This feature of our model, together with the magnitude of the relaxation time, appears to be in good agreement with the experimental results especially for the blends with $M = 31.5 \times 10^4$. Thus, from Figures 8–10, it seems that our model may give somewhat better agreement with the experimental results than Graessley's model. However, at present, the amount of data available is insufficient to claim this definitively. A more extensive test of the models would be desirable, especially for dilute blends with M_s approaching M from below.

Monodisperse Systems. Using the Graessley parameter, z, determined for the blends, we can compare the experimental data and the prediction of the two models for monodisperse systems. Figures 11 and 12 show some results of this comparison.

Figure 11 compares data for storage and loss moduli of monodisperse PS (in the melt state)[15] with the predictions of the models (with $z = 3.5$). For smaller M ($=8.85 \times 10^4$), the predictions of our model (solid lines) and Graessley's model (dotted lines) are not very different and are fairly close to the experimental data (unfilled circles). However, for larger M ($=42.7 \times 10^4$), neither gives satisfactory agreement: Although the low-frequency end of G'' of the Graessley model appears to be in fairly good agreement with the data, we note that the location of the peak in the G'' curve is significantly different for this model and the data. On the other hand, for our model, the shape of the G'' curve is much sharper (corresponding to smaller J_eG_0) relative to the experimental curve. Thus, for high molecular weight monodisperse systems, a combination of constraint release and reptation alone (in either our way or Graessley's way) is insufficient to explain the experimental data completely.

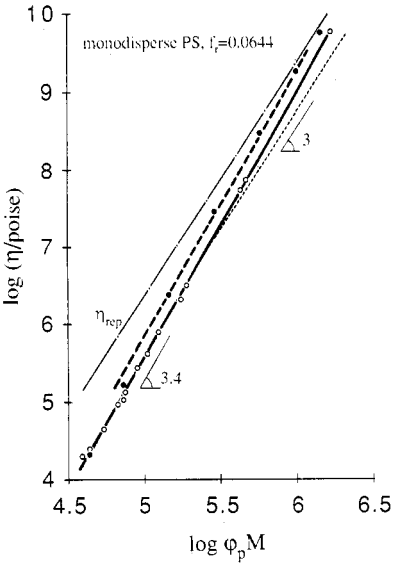

Figure 12. Comparison of the viscosity data[15,16,18] of monodisperse PS (unfilled circles) with the prediction of our CDCR model (filled circles) and the Graessley model (thin dotted line). The data for melt PS and 60% solutions in dibutyl phthalate (DBP) are reduced at the iso-friction state ($f_r = 0.0644$) and plotted against the reduced molecular weight, $\varphi_p M$. A small correction for the intensity factor of viscosity ($\propto T$) was made for both theoretical predictions and data for the PS/DBP solutions,[16] so that the results for melt and solutions can be compared in the same figure.

Figure 12 compares the experimental data for the viscosity, η, of PS (unfilled circles) with the prediction of our model (filled circles) and the Graessley model (thin dotted line). The data[15,16,18] for melt PS and PS/DBP solutions with $\varphi_p = 60\%$ were reduced to an iso-friction state and plotted against $\varphi_p M$ ($\propto M/M_e$).

As can be seen from Figure 12, η predicted by the Graessley model appears to agree well with the data for $\varphi_p M < 20 \times 10^4$ but becomes proportional to $(\varphi_p M)^3$ for $\varphi_p M > 20 \times 10^4$. We also note that η predicted by the Graessley model becomes *smaller* than the data at high molecular weight ($\varphi_p M > 30 \times 10^4$). Since the contour length fluctuation (which would be also important for monodisperse systems) is not incorporated in the model, the model prediction should still give an upper bound for the empirical data. (Note that the predicted η value would decrease if we incorporate contour length fluctuation into the model, as can be seen for Doi's theory.[11]) Thus, η for highly entangled monodisperse systems predicted by the Graessley model appears to be too small.

On the other hand, for our model, the predicted η is 2–2.5 times larger than the data, but the M dependence can be approximated by $M^{3.4}$ (thick broken line) in a fairly wide range $10 < 10^{-4}\varphi_p M < 100$. If we incorporate an additional competing mechanism (such as contour length fluctuation), the model prediction would move closer to the experimental data.

Nonmechanical Properties

According to the molecular picture (deformation of tube and successive reptation, Figure 1) we have developed, some nonmechanical properties can be calculated, to augment the viscoelastic properties discussed above. (The results obtained below remain the same even if we assume that reptation takes place first and constraint release follows it in a certain period of time.)

Diffusion. We assume the chain to take the *Gaussian* (equilibrium) conformation at time t. In a certain period of time, $t - (t + \Delta t)$, the tube composed of N_s-mers first moves according to the Rouse dynamics. For this step, the

displacement $\Delta\mathbf{R}_G^{tube}$ of the center of mass (CM), which is the same for the tube and the chain (N-mer) trapped in it, is characterized as

$$\langle \Delta\mathbf{R}_G^{tube} \rangle = \mathbf{0} \qquad \langle [\Delta\mathbf{R}_G^{tube}]^2 \rangle = 6kT\Delta t/N\zeta_t \tag{34}$$

After this step, the conformation of the tube (and the chain trapped in it) is still Gaussian. Thus, the displacement of the CM due to successive reptation step can be calculated as

$$\langle \Delta\mathbf{R}_G^{rep} \rangle = \mathbf{0} \qquad \langle [\Delta\mathbf{R}_G^{rep}]^2 \rangle = 2kT\Delta t/N^2\zeta_0 \tag{35}$$

Since the distribution of chain configuration at the beginning of the second step (reptation) is Gaussian and *not* affected by the first step (constraint release), the (distribution of) displacement of CM during the second step, which is determined only by the initial configuration for that step, has no correlation with that during the first step, i.e., $\langle \Delta\mathbf{R}_G^{tube} \cdot \Delta\mathbf{R}_G^{rep} \rangle = 0$. Thus, for the combined constraint release plus reptation processes, the diffusion coefficient of dilute N-mer in the matrix of N_s-mers is given by

$$\begin{aligned} D_G &= \langle [\Delta\mathbf{R}_G^{tube} + \Delta\mathbf{R}_G^{rep}]^2 \rangle / 6\Delta t \\ &= [(kT/N\zeta_t) + (kT/3N^2\zeta_0)] \\ &= (kT/N\zeta_0)[(\pi^2/12\Lambda N_s^3) + (1/3N)] \end{aligned} \tag{36}$$

which is identical with Graessley's result.[6] Green and co-workers[22] showed that this equation describes well the diffusion coefficient for PS/PS melt blends.

Here, we should note the essential difference between diffusion and mechanical relaxation processes described by our model (which assumes successive two steps in a short period of time). As described above, for diffusion processes, the distribution of chain configuration at the beginning of the second step is *not* affected by the first step. On the other hand, as discussed in the previous section, the chain orientation at the beginning of the second step *is* affected by the first step for the mechanical relaxation process. This is why our CDCR model predicts a $\mu(t)$ very different from that of the Graessley model. It is also the reason why the molecular weight dependence of the "diffusion relaxation time", $\langle \mathbf{R}^2 \rangle / D_G$ with $\langle \mathbf{R}^2 \rangle$ being the mean-square end-to-end distance, is different from that of the mechanical relaxation time, τ_1.[34] (For example, the M dependence of $\langle \mathbf{R}^2 \rangle / D_G$ for monodisperse systems predicted by eq 36 with $z = 3$ is very close to M^3 for M/M_e $(=N) > 10$, while τ_1 predicted by our model (with $z = 3$) can be approximated by a power-law relation, $\tau_1 \propto M^{3.2}$, for $100 > M/M_e > 10$, as shown in Figure 6.)

End-to-End Vector Correlation. Using the tangent vector $\mathbf{u}(n, t) = \partial\mathbf{r}(n, t)/\partial n$, we can define the correlation function

$$C(n, t) = \langle \mathbf{u}(n, t) \cdot \mathbf{R}(0) \rangle \tag{37}$$

where $\mathbf{R}(0)$ is the end-to-end vector at $t = 0$. The boundary condition for C is

$$C(n, t) = 0 \quad \text{at} \quad n = 0, N \quad \text{(random orientation at chain ends)} \tag{38}$$

The eigenfunctions for $C(n, t)$ with this boundary condition are given by $\sin \lambda_p n$ ($p = 1$, 2, etc.) for both constraint release (Rouse) and reptation mechanisms. Using these eigenfunctions, we obtain the time evolution of C for our CDCR model as follows.

During the period of time $t - (t + \Delta t)$, C first becomes

$$C_{tube} = \sum_q \left[(2/N) \int_0^N dn'\, C(n', t) \sin \lambda_q n' \right] \times \exp(-D_t \lambda_q^2 \Delta t) \sin \lambda_q n \tag{39}$$

due to constraint release, and further changes to

$$C(n, t+\Delta t) = \sum_p \left[(2/N) \int_0^N dn'\, C_{tube} \sin \lambda_p n' \right] \exp(-D_c \lambda_p^2 \Delta t) \sin \lambda_p n \tag{40}$$

due to successive reptation. Thus, in the limit $\Delta t \to 0$, we have

$$\partial C(n, t)/\partial t = [D_c + D_t]\, \partial^2 C(n, t)/\partial n^2 \tag{41}$$

which gives (with the boundary condition eq 38)

$$C(n, t) = \sum_p (2/N) \left[\int_0^N dn'\, C(n', 0) \sin \lambda_p n' \right] \times \exp[-(D_c + D_t)\lambda_p^2 t] \sin \lambda_p n \tag{42}$$

Note that the time-evolution equation, eq 41, is based on the rigorous Rouse dynamics (without the diagonal dominance approximation), differing from eq 19 for $S(n, t)$ described in the previous section.

If the chain assumes the equilibrium conformation at $t = 0$, we have

$$C(n, 0) = a^2 \qquad \text{for} \quad 0 < n < N \tag{43}$$

which gives

$$C(n, t) = a^2 \sum_{p=\text{odd}} (4/p\pi) \exp[-(D_c + D_t)\lambda_p^2 t] \sin \lambda_p n \tag{44}$$

Now, the end-to-end vector correlation function, $V(t) = \langle \mathbf{R}(t) \cdot \mathbf{R}(0) \rangle$, is given by[35]

$$\begin{aligned} V(t) &= \int_0^N dn\, C(n, t) \\ &= Na^2 \sum_{p=\text{odd}} (8/p^2\pi^2) \exp[-(D_c + D_t)\lambda_p^2 t] \end{aligned} \tag{45}$$

Thus, in our model, constraint release competing with reptation shifts the characteristic time but does not affect the distribution of the relaxation modes for end-to-end vector correlation. (This is because the eigenfunctions for C are the same for both mechanisms.)

It would be interesting to compare eq 45 with $V(t)$ predicted by the extended Graessley model. With assumptions 1 and 2 described earlier for the extended Graessley model, we obtain the time-evolution equation for C as

$$\partial C(n, t)/\partial t = D_c\, \partial^2 C(n, t)/\partial n^2 + k'_{cr}(t)\, C(n, t) \tag{46}$$

where the rate constant for the *uniform* constraint release is given by

$$k'_{cr}(t) = [d\nu_{cr}(t)/dt]/\nu_{cr}(t) \tag{47}$$

with

$$\nu_{cr}(t) = \sum_{q=\text{odd}} (8/q^2\pi^2) \exp(-D_t \lambda_q^2 t) \tag{48}$$

being the reduced correlation function for a *pure* constraint release process. Under the boundary and initial conditions given by eq 38 and 43, we obtain, from eq 46,

$$C(n, t) = a^2 \nu_{cr}(t) \sum_{p=\text{odd}} (4/p\pi) \exp(-D_c \lambda_p^2 t) \sin \lambda_p n \tag{49}$$

which gives

$$V(t) = Na^2 \nu_{cr}(t) \nu_{rep}(t) \qquad \text{(Graessley model)} \tag{50}$$

with

$$\nu_{rep}(t) = \sum_{p=\text{odd}} (8/p^2\pi^2) \exp(-D_c \lambda_p^2 t) \tag{51}$$

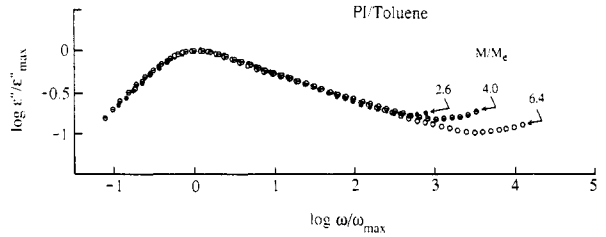

Figure 13. Frequency (ω) dependence of dielectric loss ϵ'' for *cis*-polyisoprene (PI) solutions in toluene obtained by Imanishi et al.[10] Three ϵ'' curves were shifted along the log ϵ'' and log ω axes, so that the maxima (ϵ''_{max} at ω_{max}) in those curves are superposed to compare the shape of ϵ'' curves (to illustrate the correspondence of the mode distribution of $V(t)$): M_w and M_w/M_n ratio for the PI sample are 3.16×10^4 and 1.05, respectively. The M/M_e ratio was varied by changing the concentration of PI (100%, 62%, 41% PI corresponding to $M/M_e = 6.4, 4.0, 2.6$, respectively). The increase in ϵ'' at high frequencies is attributed to the (local) segment mode due to component of dipole perpendicular to the chain contour, not to the large-scale normal mode (due to parallel component of the dipole) described by $V(t)$.

Note that the independence assumption in the original Graessley model leads to the equation

$$dV/dt = [d\nu_{rep}/dt]V_{cr} + [d\nu_{cr}/dt]V_{rep} \quad (52)$$

where V_{cr} and V_{rep} are the end-to-end vector correlation functions for pure constraint release and reptation processes, respectively. Equation 50 can be directly derived also from eq 52.

Equation 50 indicates that the relaxation mode distribution for $V(t)$ changes as the contribution of constraint release changes. This feature of the Graessley model is essentially different from that of our model, although the characteristic time $N^2/[\pi^2(D_c + D_t)]$ for $V(t)$ is the same for the two models. This difference, which would be observed whenever the contribution of constraint release changes, can be used to distinguish the two models experimentally.

For polymers having the (component of) permanent dipole moments parallel to the chain contour, the polarization of the system (due to those parallel components) is proportional to the average of the end-to-end vector of chains, and we can determine $V(t)/V(0)$ (or its Fourier transform) by dielectric measurements:[9,10] For example, the dielectric loss, ϵ'' (due to end-to-end vector fluctuation), is related to $V(t)$ as

$$\epsilon''(\omega) = \Delta\epsilon \int_0^\infty \{-d[V(t)/V(0)]/dt\} \sin \omega t \, dt \quad (53)$$

where $\Delta\epsilon$ is the dielectric relaxation intensity.

Recent experiments on *monodisperse cis*-polyisoprenes[10] (which have parallel dipole components) revealed that the shape of the dielectric spectrum (corresponding to the mode distribution for $V(t)$; cf., eq 53) in *the long time region* is *insensitive* to the M/M_e ratio, as typically shown in Figure 13. For polymers entangling not very heavily, i.e., for those with $2M_e < M < 7M_e$ shown in Figure 13, both reptation and constraint release mechanisms would largely contribute to the dynamics of the chains, and the contribution of the latter would decrease with increasing M/M_e ratio. Thus, although the effect of contour length fluctuation which should also contribute to $V(t)$ in that range of M is not clear, the above observation appears to be in better agreement with the prediction of our model (eq 45), rather than that of the Graessley model (eq 50).

Concluding Remarks

In a general vein, we believe that the value of the model we have presented here is 2-fold. First, in our view, the way we have analyzed the combined constaint release plus reptation process is straightforward and avoids making the assumption of independence of reptation and constraint release in the calculation of the dynamic quantities. The predictions are distinct from those of the Graessley model, both for the stress relaxation behavior and for the chain dynamics. In particular, for blends in the course of stress relaxation (Figures 4 and 5), our CDCR model predicts substantially more relaxation near the chain ends, a prediction that can be examined via carefully designed experiments, as well as by molecular dynamics simulations for a system of macromolecules which are long and dense enough.[36] Second, our model has some of the same characteristics as Doi's path length fluctuation model,[11] in that the CDCR model introduces a relaxation mechanism in addition to reptation that becomes progressively less important as molecular weight increases above the critical molecular weight for entanglement. As Figure 12 shows, this model for monodisperse systems, like Doi's, can mimic the experimental 3.4-th power law dependence for viscosity (as well as for relaxation time, cf., Figure 6), although the agreement for the magnitude is not very satisfactory. To our minds, this observation lends support to the notion the experimental 3.4-th power law is due to relaxation processes that are important near the onset of entanglement and gradually die out with increasing molecular weight.

Acknowledgment. We acknowledge, with thanks, stimulating discussions with Professor W. W. Graessley, Professor D. S. Pearson, and Dr. M. Rubinstein. We also thank Professor T. Kotaka, who generously allowed us to use the dielectric data for the PI/toluene systems. Financial support from the National Science Foundation, Presidential Young Investigator Program, was essential for this work and is greatly appreciated.

Appendix A

We can describe the correlation of segment orientations at nth and n'th segments by

$$S_2(n, n'; t) = \langle u_x(n, t) u_y(n', t) \rangle / a^2 \quad (A1)$$

From the boundary condition

$$S_2 = 0 \quad \text{at } n = 0, N, \quad n' = 0, N \quad \text{(random orientation at chain ends)} \quad (A2)$$

S_2 can be written as (including both diagonal and off-diagonal Rouse eigenfunctions)

$$S_2(n, n'; t) = \sum_{p,q} A_{pq}^R(t) \sin \lambda_p n \sin \lambda_q n' \quad (A3)$$

Since both ends ($n = 0, N$) of the chain are identical during the stress relaxation process after uniform deformation at $t = 0$, we may generally assume

$$S_2(n, n'; t) = S_2(n', n; t) = S_2(N-n, N-n'; t) = S_2(N-n', N-n; t) \quad (A4)$$

which leads to

$$A_{pq}^R(t) = A_{qp}^R(t), \quad A_{pq}^R(t) = 0 \quad \text{if } p + q = \text{odd} \quad (A5)$$

The time evolution of S_2 due to the Rouse mechanism (constraint release) is given by[37]

$$S_2(n, n'; t+\Delta t) = \sum_{p,q} A_{pq}^R(t) \exp[-D_t(\lambda_p^2 + \lambda_q^2)\Delta t] \sin \lambda_p n \sin \lambda_q n' \quad (A6)$$

This gives the general expression for the time evolution of $S(n, t) = S_2(n, n; t)$ due to constraint release

$$S_{tube}(n, t+\Delta t) = \sum_p A_{pp}^R(t) \exp[-2D_t\lambda_p^2\Delta t] \sin^2 \lambda_p n + \sum_{\substack{p>q \\ p+q=\text{even}}} 2A_{pq}^R(t) \exp[-D_t(\lambda_p^2 + \lambda_q^2)\Delta t] \sin \lambda_p n \sin \lambda_q n =$$

$$\sum_p A_{pp}^R(t) \exp[-2D_t\lambda_p^2\Delta t] \sin^2 \lambda_p n + \sum_{\substack{p>q \\ p+q=\text{even}}} 2A_{pq}^R(t) \exp[-D_t(\lambda_p^2 + \lambda_q^2)\Delta t] \times \sin^2 (\lambda_p + \lambda_q)n/2 - \sum_{\substack{p>q \\ p+q=\text{even}}} 2A_{pq}^R(t) \times \exp[-D_t(\lambda_p^2 + \lambda_q^2)\Delta t] \sin^2 (\lambda_p - \lambda_q)n/2 \quad (A7)$$

where we used the symmetry condition (eq A5). On the other hand, for the general expression $S(n, t) = \sum_p A_{pp}^R(t) \sin^2 \lambda_p n + \sum_{p>q, p+q=\text{even}} 2A_{pq}^R(t) \sin \lambda_p n \sin \lambda_q n$, S_{tube} obtained by eq 14 and 16 is

$$S_{tube} = \sum_p A_{pp}^R(t) \exp[-2D_t\lambda_p^2\Delta t] \sin^2 \lambda_p n + \sum_{\substack{p>q \\ p+q=\text{even}}} 2A_{pq}^R(t) \exp[-D_t(\lambda_p + \lambda_q)^2\Delta t/2] \times \sin^2 (\lambda_p + \lambda_q)n/2 - \sum_{\substack{p>q \\ p+q=\text{even}}} 2A_{pq}^R(t) \times \exp[-D_t(\lambda_p - \lambda_q)^2\Delta t/2] \sin^2 (\lambda_p - \lambda_q)n/2 \quad (A8)$$

Comparing eq A7 (rigorous Rouse dynamics) and A8 (the approximate expression used in this study), we note that the decay of the amplitude for the first terms (A_{pp}^R) is the same in eq A7 and A8, while that for the second and third terms (A_{pq}^R) is slower in eq A8. (Note that $1 > \exp[-D_t(\lambda_p \pm \lambda_q)^2)\Delta t/2] > \exp[-D_t(\lambda_p^2 + \lambda_q^2)\Delta t] > 0$). Thus, the effect of the constraint release estimated by eq 16 (and hence by eq 19) would be *smaller* than that expected from the rigorous Rouse dynamics.

Appendix B

We may write the solution of eq 19 as

$$S(n, t) = \sum_p B^*_p f_p(n) \exp[-D(2\theta_p/N)^2 t] \quad (B1)$$

where $f_p(n)$ is the pth order eigenfunction satisfying the equation

$$f_p''(n) - w\left[f_p'(0) - f_p'(N) + \int_0^N dn' Q(n') f_p''(n')\right] = -(2\theta_p/N)^2 f_p(n) \quad (B2)$$

(with $f_p' = df_p(n)/dn$ and $f_p'' = d^2f_p(n)/dn^2$) and the boundary condition

$$f_p(n) = 0 \quad \text{at} \quad n = 0, N \quad (B3)$$

Since $S(n, t)$ is symmetric, i.e., $S(n, t) = S(N-n, t)$ (cf., Appendix A), only symmetric eigenfunctions contribute to $S(n, t)$.

From eq B2 and B3, the symmetric eigenfunctions are obtained as

$$f_p(n) = (N/2\theta_p) f_p'(0) \times [\sin (2\theta_p n/N) - \{1 - \cos (2\theta_p n/N)\} \cot \theta_p] \quad (B4)$$

with

$$\tan \theta_p = -(2\theta_p/N) f_p'(0)/(wI_p) \quad (B5)$$

and

$$I_p = f_p'(0) - f_p'(N) + \int_0^N dn' Q(n') f_p''(n') \quad (B5')$$

From eq B4, I_p is calculated as

$$I_p = 2f_p'(0) + f_p'(0)(2\theta_p/N)^2(N/2\pi^2) \sum_{q=1}^N 1/[q^2 - (\theta_p/\pi)^2] \cong 2f_p'(0) + f_p'(0)(2\theta_p/N)^2(N/4)[(1/\theta_p)^2 - (1/\theta_p) \cot \theta_p] \quad \text{for} \quad N \gg 1 \quad (B6)$$

where the equality $\lim_{N\to\infty} \sum_{q=1}^N 1/[q^2 - x^2] = (1/2x^2) - (\pi/2x) \cot \pi x$ was used. Thus, from eq B5 and B6, we obtain the eigenvalue equation

$$\tan \theta_p = [(w - 2)/w]\theta_p/(2N + 1) \quad (B7)$$

For the eigenfunctions (with $f_p'(0)$ being chosen to be $(2\theta_p/N) \sin \theta_p$; cf. eq B4)

$$f_p(n) = \cos [\theta_p(2n - N)/N] - \cos \theta_p \quad (B8)$$

the orthogonality relation

$$\int_0^N dn\, f_p(n) f_q(n) - (X/N)\left\{\int_0^N dn\, f_p(n)\right\} \times \left\{\int_0^N dn\, f_q(n)\right\} = (N/2X)[(1 - X) \cos^2 \theta_p + X]\delta_{pq} \quad (B9)$$

with

$$X = w(2N + 1)/[w(2N + 1) + (2 - w)] \quad (B10)$$

holds. Applying this relation to the initial condition (cf., eq 2)

$$S(n, 0) = S_0 \text{ (constant)} \quad \text{for} \quad 0 < n < N \quad (B11)$$

we may determine the amplitude factor, B^*_p, as

$$B^*_p = -2S_0(1 - X) \cos \theta_p/[(1 - X) \cos^2 \theta_p + X] \quad p = 1, 2, ..., \infty \quad (B12)$$

Thus, eq B1, B7, B8, and B12 give $S(n, t)$ for infinitely large N.

For large but finite N, however, we should not use all eigenfunctions (f_p with $p = 1, 2, ..., \infty$) but should use N eigenfunctions, f_p, with $p = 1, 2, ..., N$, because of the physical requirement that the number of normal modes is equal to the number of segments (or, more precisely, bonds connecting the segments in our chain). A high-frequency (or short-time) cut-off is introduced by this restriction for p, which is again physically reasonable because only the long-time behavior of the chain can be described by our model. Then, we need an additional factor C^*; i.e,

$$S(n, t) = C^* \sum_{p=1}^N B^*_p f_p(n) \exp[-D(2\theta_p/N)^2 t] \quad (B13)$$

where the ratios of amplitudes of eigenfunction remain the same as those in eq B1 and B12, so that the initial condition, $S(n, 0)$ = constant, is satisfied at the scale of n larger than the segment size ($n = 1$). Local fluctuation with wavelength < 1 (segment size) and amplitude $\sim O(1/N)$ remaining in $S(n, 0)$ composed of N eigenfunctions (eq B13) has no physical meaning.

C^* can be determined by the requirement

$$\int_0^N dn\, S(n, 0) = NS_0 = C^* \sum_{p=1}^N B^*_p \int_0^N dn\, f_p(n) \quad (B14)$$

which gives

$$C^* = [\sum_{p=1}^N (2/X)(1 - X) \cos^2 \theta_p/\{(1 - X) \cos^2 \theta_p + X\}]^{-1} \quad (B15)$$

Thus, we finally obtain

$$S(n, t) = S_0 \sum_{p=1}^{N} B_p\{\cos [\theta_p(2n - N)/N] - \cos \theta_p\} \exp[-D(2\theta_p/N)^2 t] \quad \text{(B16)}$$

with

$$B_p = -Bw(2N + 1) \cos \theta_p/[w(2N + 1) + (2 - w) \cos^2 \theta_p] \qquad p = 1, 2, ..., N \quad \text{(B17)}$$

and

$$B = [\{w(2N + 1) + (2 - w)\} \sum_{k=1}^{N} \{\cos^2 \theta_k/[w(2N + 1) + (2 - w) \cos^2 \theta_k]\}]^{-1} \quad \text{(B18)}$$

In the aymptotic limit $w \to 2$ ($D_t/D_c \to \infty$), we note, from eq B7, B8, and B17, that

$$\theta_p \to p\pi \qquad B_p f_p(n) \to (2/N) \sin^2 (p\pi n/N) \quad \text{(B19)}$$

and the Rouse eigenvalues and eigenfunctions are recovered. In the another limit, $w \to 0$ ($D_t/D_c \to 0$), we see, again from eq B7, that

$$\theta_p \to (p - 1/2)\pi \quad \text{(B20)}$$

$$[\cos \theta_p/w(2N + 1)]^2 = [w(2N + 1)]^{-2}[1 + \tan^2 \theta_p]^{-1} = [\{w(2N + 1)\}^2 + \{(2 - w)\theta_p\}^2]^{-1} \to 1/(2p - 1)^2\pi^2 \quad \text{(B21)}$$

and

$$B_p f_p(n) \to [\sum_{k=1}^{N} 1/(2k - 1)^2]^{-1}[\pi/(4p - 2)] \sin (2p - 1)\pi n/N \cong [4/(2p - 1)\pi] \sin (2p - 1)\pi n/N \quad \text{(B22)}$$

(Note that $\sum_{k=1}^{N} 1/(2k - 1)^2$ converges to $\pi^2/8$ rapidly with increasing N: The difference is less than 2% for $N > 10$.) Thus, reptation eigenfunctions and eigenvalues are recovered for large N.

Registry No. PS, 9003-53-6; PI, 9003-31-0.

References and Notes

(1) Ferry, J. D. *Viscoelastic Properties of Polymers*, 3rd ed.; Wiley: New York, 1980.
(2) Graessley, W. W. *Adv. Polym. Sci.* **1974**, *16*, 1. Pearson, D. S. *Rubber Chem. Technol.* **1987**, *60*, 440.
(3) Doi, M.; Edwards, S. F. *The Theory of Polymer Dynamics*; Clarendon: Oxford, 1986.
(4) Doi, M.; Edwards, S. F. *J. Chem. Soc., Faraday Trans. 2* **1978**, *74*, 1789, 1802, 1818; **1979**, *75*, 38.
(5) See, for example: Osaki, K.; Doi, M. *Polym. Eng. Rev.* **1984**, *4*, 35.
(6) Graessley, W. W. *Adv. Polym. Sci.* **1982**, *47*, 68.
(7) Klein, J. *Macromolecules* **1986**, *19*, 105.
(8) Prager, S.; Tirrell, M. *J. Chem. Phys.* **1981**, *75*, 5194. Kim, Y. H.; Wool, R. P. *Macromolecules* **1983**, *16*, 1115.
(9) Adachi, K.; Kotaka, T. *Macromolecules* **1985**, *18*, 466.
(10) Imanishi, Y. M.S. Dissertation, Osaka University, 1987. Imanishi, Y.; Adachi, K.; Kotaka, T., to be submitted for publication in *J. Chem. Soc., Faraday Trans 1*.
(11) Doi, M. *J. Polym. Sci., Polym. Phys. Ed.* **1983**, *21*, 667.
(12) Klein, J. *Macromolecules* **1978**, *11*, 852.
(13) Daoud, M.; DeGennes, P. G. *J. Polym. Sci., Polym. Phys. Ed.* **1979**, *17*, 1971.
(14) Watanabe, H.; Kotaka, T. *Macromolecules* **1984**, *17*, 2316.
(15) Watanabe, H.; Sakamoto, T.; Kotaka, T. *Macromolecules* **1985**, *18*, 1008, 1436.
(16) Watanabe, H.; Kotaka, T. *Macromolecules* **1986**, *19*, 2520.
(17) Watanabe, H.; Kotaka, T. *Macromolecules* **1987**, *20*, 530.
(18) Watanabe, H.; Yoshida, H.; Kotaka, T. *Macromolecules* **1988**, *21*, 2175.
(19) Montfort, J. P.; Marin, G.; Monge, P. *Macromolecules* **1984**, *17*, 1551.
(20) Struglinski, M. J.; Graessley, W. W. *Macromolecules* **1985**, *18*, 2630.
(21) Roovers, J. *Macromolecules* **1987**, *20*, 148.
(22) Green, P. F.; Mills, P. J.; Palmstrøm, C. J.; Mayer, J. W.; Kramer, E. J. *Phys. Rev. Lett.* **1984**, *53*, 2145.
(23) Green, P. F.; Kramer, E. J. *Macromolecules* **1986**, *19*, 1108.
(24) Antonietti, M.; Coutandin, J.; Grütter, R.; Sillescu, H. *Macromolecules* **1984**, *17*, 798.
(25) Antonietti, M.; Coutandin, J.; Sillescu, H. *Macromolecules* **1986**, *19*, 793.
(26) Note that eq 19 is not the general time-evolution equation for arbitrary boundary conditions, because the particular boundary condition ($S = 0$ at $n = 0, N$; eq 9) is already used in eq 18.
(27) This expression (eq 27) was first obtained by Klein.[12]
(28) If we apply eq 24′ (our model) and 27 (Graessley model) to experimentally obtained τ_1 to estimate τ_{tube}, the latter gives *apparent* N_e dependence of τ_{tube} much weaker than that obtained from the former.
(29) If we use the initial condition eq 2b for $S(n, t)$, we reach the relation of rubber elasticity $G_0 = cRT/M_e$. This relation leads to the asymptotic J_e^R value being very close to the Rouse value (=0.4), instead of that (≃0.5) found in Table II.
(30) It is important that τ_1 exhibits the power law dependence on N_e only in the asymptotic and universal region where the compliance of the N-mer is independent of N_e. This fact was successfully used to estimate the N_e dependence of τ_1 experimentally, and the relation $\tau_1 \propto N_e^3$ was confirmed.[18]
(31) Rubinstein, M.; Helfand, E.; Pearson, D. S. *Macromolecules* **1987**, *20*, 822.
(32) Note that the opposite is not necessarily true for blends with $M \sim M_e$: If the lifetime of the entanglement between the longer and shorter chains is comparable with that for the entanglement between longer chains, we hardly observe stronger φ_L dependence even for blends containing those two kinds of entanglements.
(33) We found that the terminal relaxation intensity of the $G'_{L,B}$ curve for the blends with $M = 270 \times 10^4$ and $\varphi_L = 2\%$ reported by Montfort et al.[19] was significantly higher than the model prediction, probably because of the entanglement between the longer chains. To examine this point, we used the η_B and $\eta_{S,m}$ data for a series of blends with $M = 270 \times 10^4$, $M_s = 10 \times 10^4$, and $2 \le \varphi_L$ (%) ≤ 31 reported in their paper[19] and evaluated $\eta_{L,B}$ (cf., eq 30b). We found that $\eta_{L,B}$ for those blends exhibited a φ_L dependence significantly stronger than that described by eq 30e in the range $\varphi_L \ge 2\%$, suggesting the longer chains (with $M = 270 \times 10^4$) to be still entangled with themselves in the blends to some extent even at $\varphi_L = 2\%$. (In fact, the critical φ_L value for the onset of entanglements between the longer chains with nearly the same length ($M = 281 \times 10^4$) was found to be somewhere between 1 and 2%.[15])
(34) In this connection, for monodisperse systems, we note that the difference between the N dependence of τ_1 and that of $\langle \mathbf{R}^2 \rangle / D_G$ is larger in our model than in Graessley model.
(35) From the physical requirement discussed in Appendix B, the sum in eq 45 (and eq 44) should be taken for $1 \le p(\text{odd}) \le (2N - 1)$. However, for $C(n, t)$ and $V(t)$, the correction due to this cut-off for p is very small for sufficiently large N, as also shown in Appendix B. We also note that correction does not change the distribution (i.e., relative magnitudes) of intensities of slow normal modes even if N is not sufficiently large. Thus, the discussion for Figure 13 does not change.
(36) Grest, G. S.; Kremer, K.; Carmesin, I. *Bull. Am. Phys. Soc.* **1988**, *33*, 445.
(37) For $S_2(n, n'; t)$, we can write the rigorous time-evolution equation (due to constraint release and reptation) $\partial S_2(n, n'; t)/\partial t = [D_t + D_c](\partial^2/\partial n^2 + \partial^2/\partial n'^2)S_2(n, n'; t) + 2D_c\, \partial^2 S_2(n, n'; t)/\partial n \partial n'$. However, in general, this equation cannot be solved analytically. Thus, we used the diagonal dominance approximation in this study to solve the problem analytically.